

JGR Solid Earth

RESEARCH ARTICLE

10.1029/2023JB026684

Volcanic Early Warning Using Shannon Entropy: Multiple Cases of Study



Key Points:

- While successful volcanic forecasting has been achieved, there is no generally valid model suitable for large range of eruptive scenarios
- We used feature extraction to analyze seismic data from five well studied volcanoes to identify short-term eruptive precursors
- Shannon entropy has a uniform temporal pattern of pre-eruptive change and is a recurrent and transferable feature

Supporting Information:

Supporting Information may be found in the online version of this article.

Correspondence to:

J. M. Ibáñez,
jibanez@ugr.es

Citation:

Rey-Devesa, P., Benítez, C., Prudencio, J., Gutiérrez, L., Cortés-Moreno, G., Titos, M., et al. (2023). Volcanic early warning using Shannon entropy: Multiple cases of study. *Journal of Geophysical Research: Solid Earth*, 128, e2023JB026684. <https://doi.org/10.1029/2023JB026684>

Received 7 MAR 2023

Accepted 1 JUN 2023

Author Contributions:

Conceptualization: Jesús M. Ibáñez

Data curation: Pablo Rey-Devesa, Ligdamis Gutiérrez, Ivan Koulakov, Luciano Zuccarello

Formal analysis: Pablo Rey-Devesa

Funding acquisition: Carmen Benítez, Jesús M. Ibáñez

Investigation: Jesús M. Ibáñez

Methodology: Pablo Rey-Devesa, Carmen Benítez, Ivan Koulakov, Jesús M. Ibáñez

Project Administration: Jesús M. Ibáñez

Software: Pablo Rey-Devesa, Carmen Benítez, Ligdamis Gutiérrez, Guillermo Cortés-Moreno, Manuel Titos

Pablo Rey-Devesa^{1,2} , Carmen Benítez³ , Janire Prudencio^{1,2} , Ligdamis Gutiérrez^{1,2} , Guillermo Cortés-Moreno^{1,2}, Manuel Titos³, Ivan Koulakov^{4,5} , Luciano Zuccarello⁶ , and Jesús M. Ibáñez^{1,2,7} 

¹Department of Theoretical Physics and Cosmos, Science Faculty, University of Granada, Granada, Spain, ²Andalusian Institute of Geophysics, Campus de Cartuja, University of Granada, Granada, Spain, ³Department of Signal Theory, Telematics and Communication, Informatics and Telecommunication School, University of Granada, Granada, Spain, ⁴Trofimuk Institute of Petroleum Geology and Geophysics SB RAS, Novosibirsk, Russia, ⁵Institute of the Earth's Crust SB RAS, Irkutsk, Russia, ⁶Istituto Nazionale di Geofisica e Vulcanologia, Sezione di Pisa, Pisa, Italy, ⁷Istituto Nazionale di Geofisica e Vulcanologia, Sezione di Catania, Osservatorio Etneo, Catania, Italy

Abstract The search for pre-eruptive observables that can be used for short-term volcanic forecast remains a scientific challenge. Pre-eruptive patterns in seismic data are usually identified by analyzing seismic catalogs (e.g., the number and types of recorded seismic events), the evolution of seismic energy, or changes in the tensional state of the volcanic medium as a consequence of changes in the volume of the volcano. However, although successful volcanic predictions have been achieved, there is still no generally valid model suitable for a large range of eruptive scenarios. In this study, we evaluate the potential use of Shannon entropy as short-term volcanic eruption forecasting extracted from seismic signals at five well studied volcanoes (Etna, Mount St. Helens, Kilauea, Augustine, and Bezymianny). We identified temporal patterns that can be monitored as short-term eruptive precursors. We quantified the decay of Shannon entropy prior to eruptions, noting that changes appear between 4 days and 12 hr before. When Shannon entropy is combined with the temporal evolution of other features (i.e., energy, kurtosis, and the frequency index), we can elaborate physical models according to the occurring volcanic processes. Our results show that pre-eruptive variation in Shannon entropy is a confident short-term volcanic eruption monitoring tool.

Plain Language Summary Volcanic eruptions represent a major natural hazard. Despite decades of research, the forecasting of volcanic eruptions remains a scientific challenge. Subsurface volcanic processes generate seismic waves, which can be measured at the surface using seismometers. To date, the most successful examples of eruption forecasting have been based on seismic data. However, we still lack a early warning model that can be applied across the wide range of eruption styles seen around the world. In this study, we implemented a new approach for the analysis of seismo-volcanic data aimed at warning eruptions. We used advanced signal processing algorithms to analyze continuous seismic signals from a suite of well-studied volcanoes (Mount St. Helens, Mt. Etna, Kilauea, Augustine, and Bezymianny) in order to create a new database of features found within the seismic signals. We found that pre-eruptive variation in the Shannon entropy (a statistical parameter associated to the coherence of the seismic sources) of seismic signals offers a successfully feature for short-term volcanic eruption alert. The relationship between pre-eruptive seismic signals and Shannon entropy is based on changes in the probability distributions of the type of seismic waves, independent of the signal source.

1. Introduction

Volcanic eruptions impact significantly on the Earth and, in particular, on humanity, since more than 14% of the world population (more than 1 billion people) lives under the direct threat of the consequences of volcanic eruptions (Freire et al., 2019). Today, society is increasingly demanding efficient early warning protocols (e.g., W. A. Thelen et al., 2022) that are sufficiently long to allow for evacuations and/or other defense protocols, but short enough to not lose effectiveness and credibility (Whitehead & Bebbington, 2021). Forecasting volcanic eruptions relies on the ability to identify physical and chemical changes in the volcanic system based on the analysis of geophysical and geochemical time series, and in the successful implementation of such data analysis frameworks for pattern recognition in real- or quasi-real-time (e.g., Ardid et al., 2022; Caudron et al., 2020; Dempsey

© 2023. The Authors.

This is an open access article under the terms of the [Creative Commons Attribution License](https://creativecommons.org/licenses/by/4.0/), which permits use, distribution and reproduction in any medium, provided the original work is properly cited.

Supervision: Carmen Benítez, Janire Prudencio

Validation: Pablo Rey-Devesa, Carmen Benítez, Guillermo Cortés-Moreno, Ivan Koulakov, Jesús M. Ibáñez

Visualization: Janire Prudencio, Jesús M. Ibáñez

Writing – original draft: Jesús M. Ibáñez

Writing – review & editing: Pablo Rey-Devesa, Carmen Benítez, Janire Prudencio, Manuel Titos, Jesús M. Ibáñez

et al., 2020; Girona et al., 2019, 2021; Manga et al., 2017; McKee et al., 2021a, 2021b; Sparks, 2003; Sparks et al., 2012). After decades of research, the scientific community is currently having certain degree of success in providing volcanic early warnings to the relevant authorities (Cameron et al., 2018; Kilburn, 2018; Kilburn & Bell, 2022). However, due to the variety of eruptive styles, the fact that not every unrest episode ends in eruption and the incapability of most pattern recognition approaches to actually be recognized in real time, forecasting volcanic eruptions remains a challenge (e.g., Jolly et al., 2020; Manley et al., 2021).

Volcano seismology is one of the most important tools for volcano monitoring and early warning (McNutt & Roman, 2015; Power et al., 2020; Pyle, 2015; Saccorotti & Lockmet, 2021). Volcanic activity generates a variety of seismic signals that reflect multiple complex processes acting within the volcanic system (e.g., Chouet & Matoza, 2013; Ibáñez et al., 2000), including ground deformations, opening of fractures and conduits, fluids transport and eruptions. As such, seismic signals could contain crucial information for deciphering processes that control the occurrence, timing, and magnitude of eruptions. For this reason, majority forecast models are based on the use of seismic data and the search of relationship between seismo-volcanic signals, the assessment of their source mechanisms, and volcanic activity models. For example, the Generic Swarm Model (McNutt & Roman, 2015) is one of the broadly adopted models to forecasting eruptions using seismic data. In this model the main assumption is volcanic eruptions are preceded by swarms of earthquakes, long period or hybrid event sequences, and tremor. To apply this approach, the use of Machine Learning (ML) to study seismo-volcanic signals offers a unique opportunity to obtain maximum information in the shortest time (Benítez et al., 2006; Ibáñez et al., 2009; Manley et al., 2020; Martínez et al., 2021; Ren et al., 2020; Titos, Bueno, García, & Benitez, 2018; Titos et al., 2019).

Contemporaneously, other widely used forecasting models, like Failure Forecasting Systems, are fundamentally based on the assumption that an acceleration of energy represents an eruption forecast (e.g., Boué et al., 2015, 2016; Power et al., 2013). Other models include some variations of these aspects, such as implementing seismic ratios based on analyzing the energy measured in different frequency bands (Ardid et al., 2022; Bueno et al., 2019; Caudron et al., 2021; Chardot et al., 2015). Despite their widespread adoption during volcanic crises, significant shortcomings lie in the fact that these models are based on the evaluation of very few parameters (e.g., signal type, number of events). Regardless of these limitations, a number of recent studies have used ML techniques for multi-parametric interpretation of changes in the eruptive states of volcanoes in order to find predictive patterns (e.g., Manley et al., 2021). Bueno et al. (2019, 2021a) applied Bayesian Neural Network (BNN) methods to frequency analysis of seismic signals at three different volcanoes: Bezymianny, Mount St. Helens, and Mt. Etna and found that the evolution of the uncertainty offers effective eruption early warning that is transferable between volcanic systems. Furthermore, these authors highlighted the importance of analyzing the temporal evolution of seismic features instead of focusing only on the classification of isolated seismic events. Until now, the study of seismic feature evolution has mainly focused on seismic energy (i.e., the real-time seismic amplitude measurement, RSAM; (e.g., Ardid et al., 2022; Endo & Murray, 1991) or calculating the energy of earthquakes using their magnitude, their stress release, or the Material Failure Forecasting Method (e.g., Boué et al., 2015, 2016; Cornelius & Voight, 1995; Massa et al., 2016). Satisfactory results have been obtained when applied together with ML methods to obtain the completeness of seismic catalogs (e.g., Alparone et al., 2015; Cortés et al., 2009; Trujillo-Castrillón et al., 2018); however, the resulting models have not been tested to be transferable to other volcanic systems.

The optimal parametrization of a seismic signal is a crucial issue in seismic signal processing and data analysis (Alvarez et al., 2011; Cortés et al., 2015, 2019; Malfante, Dalla Mura, Mars, et al., 2018; Malfante, Dalla Mura, Métaixian, et al., 2018). Various methods have been used to transition from the original frame of reference (raw seismograms) to a feature frame. Authors extract parameters (features) from the data and use them to perform a classification of isolated seismic events (e.g., Bueno et al., 2018; Cortés et al., 2014; Titos, Bueno, García, Benítez & Ibáñez, 2018; Titos et al., 2022). These features are mainly grouped into three types according to the information they represent: (a) phenomenological features describe seismogram characteristics that are independent of the volcanic system; (b) statistical features represent statistical parameters of the waveform and its frequency content; (c) signal domain transforms that are determined by applying a transform to the waveform to characterize the signal in a different domain (e.g., in the frequency domain).

In this study, we evaluated the pre-eruptive temporal evolution of Shannon entropy for potential use as volcanic early warning. Shannon entropy is a statistical parameter that reveals how similar the seismic signal is to itself

in the frequency domain over time. Our starting hypothesis is that prior to an eruptive process, the energy of the volcanic system increases and background noise becomes irrelevant; therefore, the seismic signal should resemble itself more and more before the imminent eruption. We used signal processing techniques to analyze continuous seismic signals from five well-studied volcanoes (Mount St. Helens, Mt. Etna, Kilauea, Augustine, and Bezymianny) in order to study the evolution over time of the Shannon entropy to identify potential targets for volcanic eruption monitoring.

We are confident that performing volcano-seismic monitoring using the Shannon entropy will help to improve volcanic early warning (which is generally called volcanic forecasting) because it is: (a) self-sustaining (it has the ability to carry out volcanic warning itself); (b) agnostic (it does not need established a priori physical models); (c) simple (it is successful with only one input, the seismic signal); (d) direct (it does not need specific previous training); (e) transferable (it can be generalized for different eruptive scenarios); and (f) flexible (it can be adapted to the development of new knowledge). The method presented here can be exported to other volcanoes around the world, offering the potential for high societal impact and widespread interest among the scientific community.

2. Feature Extraction and Model Development

When characterizing seismic signal, and especially to apply ML studies on isolated seismic events, several authors have highlighted the possibility of using a large number of seismic features, even more than hundreds of them (e.g., Malfante, Dalla Mura, Mars, et al., 2018; Malfante, Dalla Mura, Métaxian, et al., 2018). After analyzing them (see Supporting Information S1), we found the temporal evolution of Shannon entropy as the most interesting to be tested as short-term forecasting feature.

We studied the temporal evolution of the Shannon entropy to determine if it is evolving in a relevant way comparing non-eruptive periods with pre-eruptive and eruptive episodes. It is calculated using the equation from below (Esmaili et al., 2004).

$$-\sum_i P(S_i) \log_2(P(S_i)) \quad (1)$$

From a statistical perspective, the Shannon entropy of seismic signals has been defined as the distribution of amplitude levels of a given signal (van Ruitenbeek et al., 2020) or a measure of uncertainty in probability distributions (Malfante, Dalla Mura, Mars, et al., 2018). van Ruitenbeek et al. (2020) suggested that amplitude levels of a periodic signal are equally likely and the entropy is high, while a single impulse within a continuous (constant amplitude) signal will have lower entropy. Malfante, Dalla Mura, Mars, et al. (2018) suggested that the maximum Shannon entropy (i.e., the maximum uncertainty) occurs where all possible outcomes have equal probabilities (i.e., a distribution characterized by maximum heterogeneity or randomness), while minimum uncertainty occurs when one possible outcome has a probability of one (i.e., there is no uncertainty and entropy is zero).

In our seismic signals, Shannon entropy represents the uncertainty of the state of the volcanic system and is related to the type of seismic signal. When the seismic signal is composed of random signals originating from different sources (i.e., very broad spectral content), Shannon entropy is high, reflecting the high uncertainty in the types and sources of waves. As such, Shannon entropy provides a quantitative estimate of the homogeneity of the volcanic process. The rapid decrease toward zero reflects a single dominant process within the time and frequency domain that generates seismic waves before an eruption. The seismic source during the eruptive process can manifest in different ways. For example, multiple fractures induce volcano tectonic (VT) earthquakes, bubbles or fluid resonance generates LP-type events, and a source sustained over time causes volcanic tremor. Each of these source processes results in different energy behaviors (the occurrence of many low energetic events might not show an increase in the energy). However, the evolution of Shannon entropy is always in the same direction; it will decrease toward zero as the state of the volcano evolves toward an eruptive and energetic process.

The workflow developed in this study is shown in Figure 1. This procedure is conceived to extract a single parametric analysis (obtaining a vector) or a multi-parametric feature study (obtaining a matrix of features). We only used the vertical component of the seismic signal because at the present many volcanoes continue being seismically controlled by one component seismometer, and one of the scopes of this work is to generalize the results. The first step is to filter the signal using a bandpass filter from 1 to 16 Hz to reduce sources of noise. Below 1 Hz, the influence of the oceanic load over the seismic signal is too strong and must be removed according to the

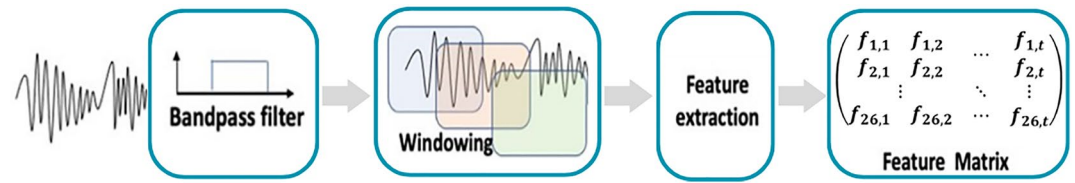


Figure 1. Schematic workflow illustrating the methodology used to transform the seismic data from the amplitude-time space of seismograms to the temporal matrix space of features.

results of Almendros et al. (2007); at frequencies of >15–20 Hz, climatic and anthropic conditions (wind, rain, traffic, etc.) affect the seismic signals. For each seismogram, selected an interval of time (1 or 10 min overlapped by 50%, according the volcano) over which the parametric transformation is computed.

As indicated above, we should expect that previous to an eruptive episode the Shannon entropy must evolve toward zero, or reaching a minimum. In order to quantify the decay of this feature we used a widely accepted algorithm such as Short Time Average (STA)/Long Time Average (LTA) (Jones & van der Baan, 2015; Trnkoczy, 2009). We estimated the mean value of the Shannon entropy for each volcano during resting periods (SE_0) and implemented small windows of analysis to calculate how the Shannon entropy was evolving ($SE(i)$) according to this resting value, using Equation 2. In average the LTA value was estimated in an interval of 20 days of volcanic repose for each volcano. The STA has the same duration of the window used to feature extraction analysis (from 1 to 10 min). We then established a threshold which allows us to forecast the eruption without having false alarms (Equation 2). When the value of the decay remains over the 70%, that is, the STA is lower than 30% of the LTA value, we consider this is the starting of the potential short term forecast interval. The value of 70% of threshold is an experimental and compromise value based on the generic value used in many research works to determine the error interval of experimental results. It is clear that increasing this value of threshold the short-term forecasting period would be reduced, but reducing it we have the chance to have several false alarms.

$$\text{Decay Ratio [\%]} = 100 \cdot \left(1 - \frac{SE(i)}{SE_0} \right) \quad (2)$$

3. Data and Volcanic Scenarios

We selected data from five well-studied volcanoes (Mt. Etna, Mount St. Helens, Augustine, Bezymianny, and Kilauea); Table 1 represents a broad range of volcanic processes and eruption styles, as long as several eruptive mechanisms, showing different pre-eruptive seismic patterns with different kind of signals (volcano-tectonic, long period, volcanic tremor, etc.). This makes this comparison among them interesting to test the exportability of our hypothesis. For each volcanic scenario, if available, we analyzed several seismic stations but here will we only present results of one station per eruptive scenario, selected based on proximity to the eruptive center and/or the completeness of the seismic catalog (Figure 2). Other stations showed similar results. We want to emphasize that the volcanoes Mt. Etna, Bezymianny and Mount St. Helen have been selected, in addition to their interest based on their eruptive history, because they were the volcanoes studied by Bueno et al. (2021a, 2021b) where it was observed how uncertainty could be used as a forecasting indicator.

The selection of the databases was conditioned on the availability of public data available online in repositories such as IRIS, or based on data acquired by our work team in temporary field campaigns or through institutional agreements (Mt. Etna and Bezymianny). The Data Availability section presents the links to access all the data used for this analysis. The eruptive processes selected for study have been selected based on different reasons: (a) relevance of the eruptions, as is the case of Augustine 2006, Mount St. Helens 2004, Kilauea, 2018; (b) have been previously analyzed using uncertainty, such as Mt. Etna, 2013, Bezymianny 2007; (c) have a long series of quality seismic records and have an eruptive event recorded on video and an eruptive column more than 11 km high, in the case of the Bezymianny 2017 volcano. Noteworthy, even if public repositories offer available volcanic seismic data, long time series of them are not always accessible and only short time intervals around some specific volcanic events are uploaded with enough quality to make the analysis feasible.

The eruption of Mount St. Helens (2004) represents the reawakening of this volcano after more than 10 years of calm (Iverson et al., 2006). Itself the size of this eruption is not too large, but it was forecasted by intense seismicity

Table 1
Volcanic Data and Seismic Stations

Volcano (location)	Period	Seismic station	Description and activity	Monitoring	References
Mt. Etna (Sicily, Italy)	11, 17, 23, 28 November 2013	EBEM	Basaltic Stratovolcano Volcanic tremor Strombolian activity and Lava Fountain	INGV-OE (Istituto Nazionale di Geofisica e Vulcanologia—Osservatorio Etneo)	Aloisi et al. (2020), Barreca et al. (2018), (2020), Bonaccorso et al. (2014), Presti et al. (2020), Spampinato et al. (2019), and Zuccarello et al. (2022)
Bezymianny (Kamchatka, Russia)	20 December 2017	BZ01 (Figure 2: blue)	Andesitic volcano	Temporary Field Experiment (2017)	Bueno et al. (2019), Davydova et al. (2022), Girina (2013), Koulakov et al. (2021), Mania et al. (2019), and W. Thelen et al. (2010)
Mount St. Helens (Washington, USA)	25 September, 14 October, 5 November 2007	BELO (Figure 2: green)	VT activity Dome growth, Very energetic explosions	KGBS (Kamchatkan Branch of Geophysical Survey)	Anderson and Segall (2013), Berlo et al. (2004), De Siena et al. (2014), Gabrielli et al. (2020), Iverson et al. (2006), Lehto et al. (2010), and Sherrod et al. (2008)
Augustine (Alaska, USA)	1 October 2004	SHW	Andesitic-Dacitic Stratovolcano VT and tremor Phreatic Eruption	Pacific Northwest Seismic Network University of Washington	Bailey et al. (2006), Buurman and West (2006), Coombs et al. (2010), DeRoin and McNutt (2012), DeShon et al. (2010), Manley et al. (2021), Power et al. (2010), and Zhan et al. (2022)
Kilauea (Hawaii, USA)	11 January 2006	AUH	Andesitic-Dacitic Stratovolcano VT activity Vulcanian activity	AVO (Alaska Volcano Observatory)	Neal et al. (2019), Patrick et al. (2020), and Roman et al. (2021)
	3 May 2018	JOKA	Basaltic Shield Volcano Summit Collapse and fissure eruptions	HVO (Hawaiian Volcano Observatory)	

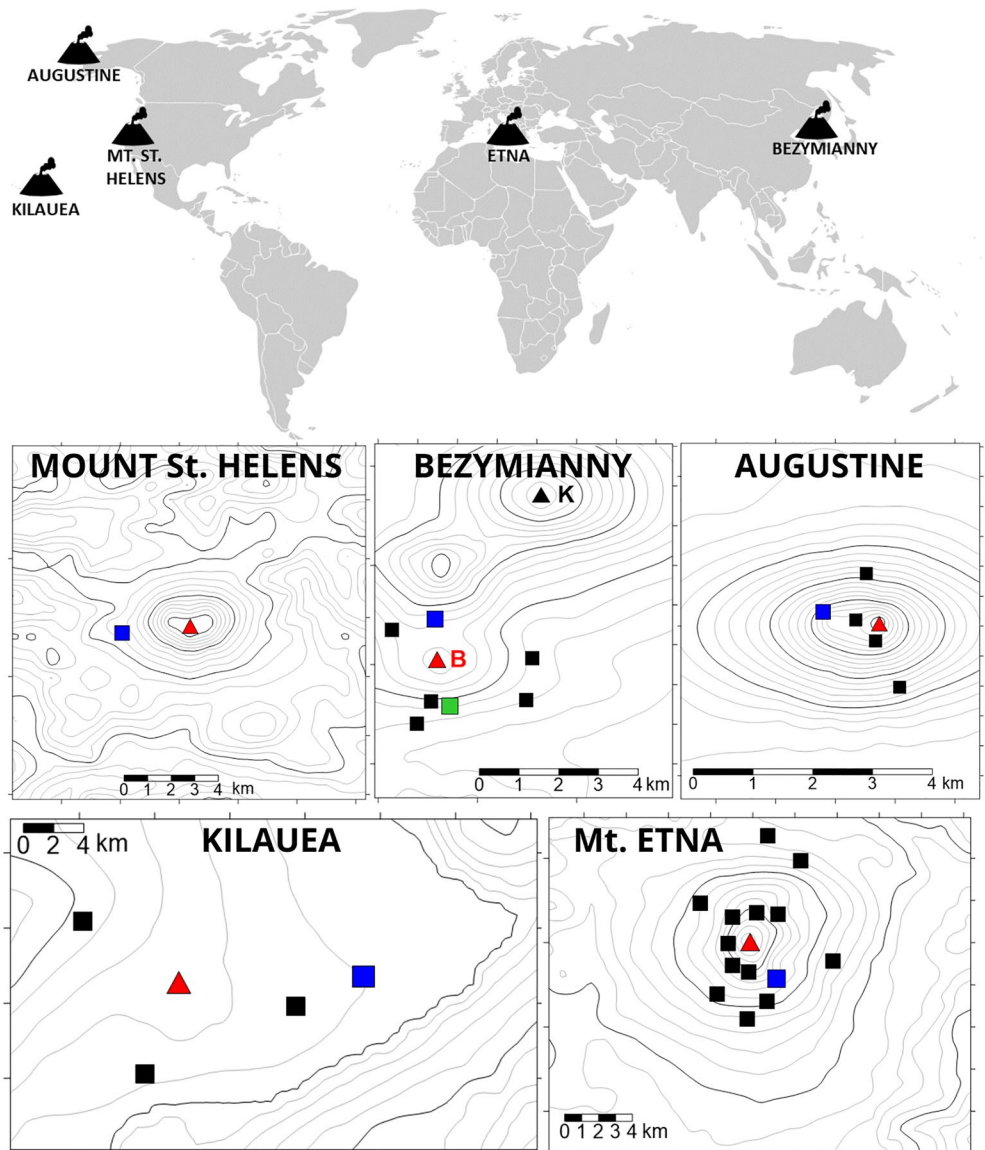


Figure 2. Study region locations and maps of the seismic networks for each of the five volcanoes: Mount St. Helens, Bezymianny, Augustine, Kilauea and Mt. Etna. Red triangles denote the main eruptive center, squares represent the used seismic stations and blue square are the seismic stations used to plot the figures of this work. In the map of the Bezymianny volcano we denoted in black triangle and with a letter K the position of the volcano Kliuchevskoy and added the letter B to the main eruptive center of Bezymianny volcano. In Bezymianny map blue square represents the station BZ01 and the green square is the station BELO.

of volcanic tectonic earthquakes and followed by an energetic volcanic tremor prior the explosion of the extruded dome. The eruption of Augustine volcano was a moderate explosion (VEI 3) with an unrest characterized by intense seismicity lasting at least 5 months prior the eruption of 11 of January 2006 (Manley et al. (2021)). This eruption is characterized by two explosions within 30 min detected by satellite observations Bailey et al. (2006), generating ash plumes to maximum heights of 6.5 and 10.2 km respectively. This eruptive phase lasted 17 days with at least 14 representative explosions. The Kilauea volcano eruption of 2018 represents a special case within the eruptive mechanism of this volcanic system. The eruption is preceded by a collapse of part of the building that occurs on the night of April 30. Several days later, on May 3, the first fissures appear with the emission of lava flows. Finally, on May 5, an earthquake of magnitude Mw 6.9 occurred on the flank of the building, which ended up opening more fissures and larger lava flows (Patrick et al., 2020). Since approximately the year 2000, the Mt Etna volcano has had a continuous eruptive activity, alternating lava flows, lava fountains and some moderate

explosive episodes (Spampinato et al., 2019). In general, seismic activity is represented by the occurrence of shallow VT earthquakes, long period events and continuous volcanic tremor (Zuccarello et al., 2022). For this analysis we have selected four episodes of lava fountains from 2013, previously studied by Bueno et al. (2021a, 2021b) and which were forecasted by a strong volcanic tremor and absence of VT earthquakes. For Bezymianny volcano we selected two eruptive phases. In the first one, in 2007, it was observed how the uncertainty always decreased prior to each of the three selected explosions, being the initial motivation of this work. In 2017 the Institute of Volcanology and Seismology of the Russian Academic of Sciences (Koulakov et al., 2021) organized a temporary seismic experiment deploying several Broad Band stations around the volcano. On 20 December 2017 a large volcanic explosion occurred with an eruptive column at least 11 km high that will be analyzed in detail later. The advantage of this experiment is that we have a full year of data available, continuously, at various stations. This will allow us to study in depth if the Shannon entropy can be considered as a recurrent and differentiable parameter as an element of short-term volcanic forecasting as Ardid et al. (2022) define to be used in a general way in early warning volcanic eruption protocols.

4. Results

The first step to ensure that the idea that the Shannon entropy is used as a reliable parameter as a forecast of volcanic eruption is to check if it meets the requirements indicated by Ardid et al. (2022). These authors define an eruption precursor as a common pattern that has to be recurrent (occurs prior to multiple events), transferable (occurs prior to eruptions at different volcanoes) and differentiable (absent during non-eruptive unrest and volcanic repose). In the following, we explain why we consider Shannon entropy a differentiable parameter.

For this analysis, it is necessary to study long time series. However, the continuous availability of data without interruptions and with the same recording system is a complex task. On the base of the advantage of the seismic experiment performed in Bezymianny volcano we have the capability to analyze a whole year of high-quality data from continuous seismic signals. In this period, we can identify both resting periods and pre-eruptive activity before the energetic explosion of 20 December 2017. We considered these data reliable enough to trust the results obtained and proceed to test the method in different eruptive episodes of this volcano, and also in different volcanoes.

Systematic analysis of Shannon entropy at Bezymianny from August 2017 to July 2018 (Figure 3) revealed that generally, the mean values obtained remain high. However, we observed some intervals in which this trend decays to lower values. As described above we defined a significant decrease of the values of the Shannon entropy when the STA value decays until more than the 70% of the LTA value. Following this rule, we detected few intervals with this pattern. The biggest decay occurred in the instant of the largest volcanic explosion of 20 December 2017 (the STA value 98.3% lower than the LTA one). In addition, low Shannon entropy values were observed on other intervals with decays lower than 70%. Analyzing data from the KBGS (Kamchatka Branch Geophysical Survey) institution two important explosions were reported at the neighboring Kliuchevskoy volcano (August 2017 and May 2018). Both eruptions are clearly aligned with the first and last drops in Shannon entropy (marked as a red shadow area in Figure 3). We suggest that these low Shannon entropy anomalies are potential forecasting evidences of the explosions at Kliuchevskoy volcano. The relatively lower value reached for the Bezymianny event may reflect the closer distance to the seismic station (BZ01 is <2 km from the summit of Bezymianny and ~10 km from the summit of Kliuchevskoy; Figure 2). The recorded Kliuchevskoy signals at BZ01 station likely suffered seismic attenuation effects and interference by local signals and other sources of noise. There is a minimum of short duration located on September 2017 associated with a local earthquake of magnitude Mw 4.3 as reported in IRIS institution. The decrease observed in March 2018 is associated to an intense volcanic tremor recorded in the volcanic area. We have no evidences of potential volcanic eruptions or lava dome growth that could be associated with this activity, but the presence of this intense volcanic tremor confirms its volcanic source. Finally, during April 2018 an intense volcano-tectonic earthquake swarm was recorded, associated with a set of three minimum values of the Shannon entropy. According to these observations, and at least for the period of time analyzed, the significant decreases in the Shannon entropy values seem to be exclusively associated with eruptive processes.

The next step is determining if this decrease in Shannon entropy values can be quantified as a promising evidence of short-term volcanic forecasting tool. In Figure 4 we show the evolution of the Shannon entropy a week prior to the explosion of 20 December 2017. The STA/LTA ratio was computed and in shadow green we highlight the instant in which the decay is continuously lower than the 70% (the vertical red line marks the instant of the

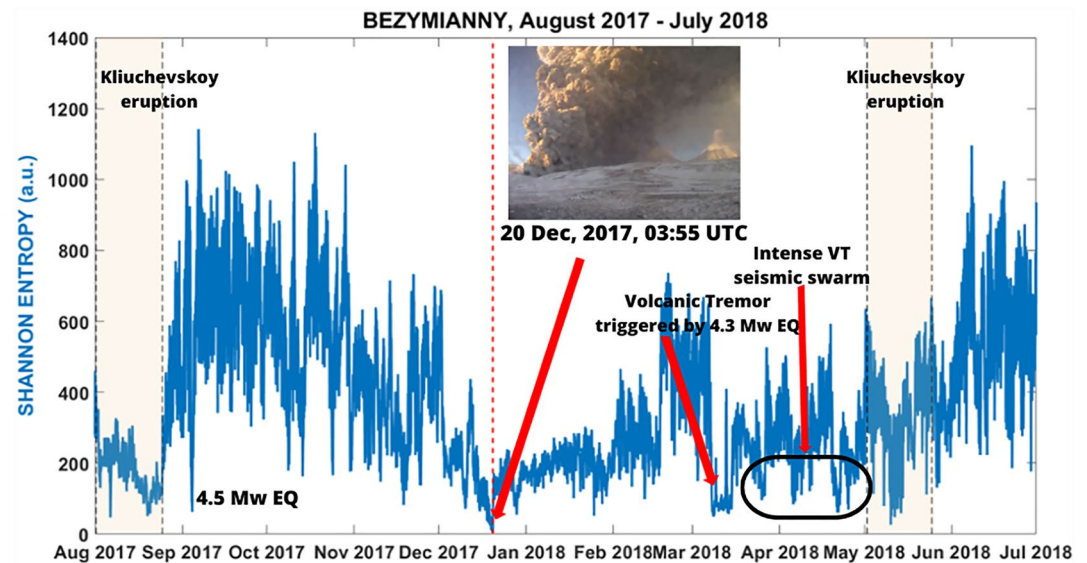


Figure 3. Temporal variation of Shannon entropy at station BZ01 of Bezymianny from August 2017 to July 2018. The biggest decay occurred in the instant of the largest volcanic explosion of 20 December 2017. Additional low Shannon entropy values were observed. Data from the KBGS (Kamchatka Branch Geophysical Survey) institution reported two important explosions at the neighboring Kliuchevskoy volcano (August 2017 and May 2018) marked as a red shadow area. There is a minimum of short duration located on September 2017 associated with a local earthquake of magnitude Mw 4.3 as reported in IRIS institution. The decrease observed in March 2018 is associated to an intense volcanic tremor recorded in the volcanic area triggered by another local earthquake of Mw 4.5 (reported in IRIS). In April 2018 an intense volcano-tectonic earthquake swarm was recorded, associated with a set of three minimum values of the Shannon entropy.

eruptive process). Notice that its continuous decay appears 2 days before the eruption, reaching values close to zero in the moment of the explosion (as indicated above a decay of 98.3%). However, as marked in Figure 4, at least 5 days before we can consider potential forecasting evidences.

Referring to the three explosions of the Bezymianny volcano in 2007, this same procedure for estimating the decay of the STA/LTA ratio of the Shannon entropy was repeated. In Figure 5 we plot these results. As observed

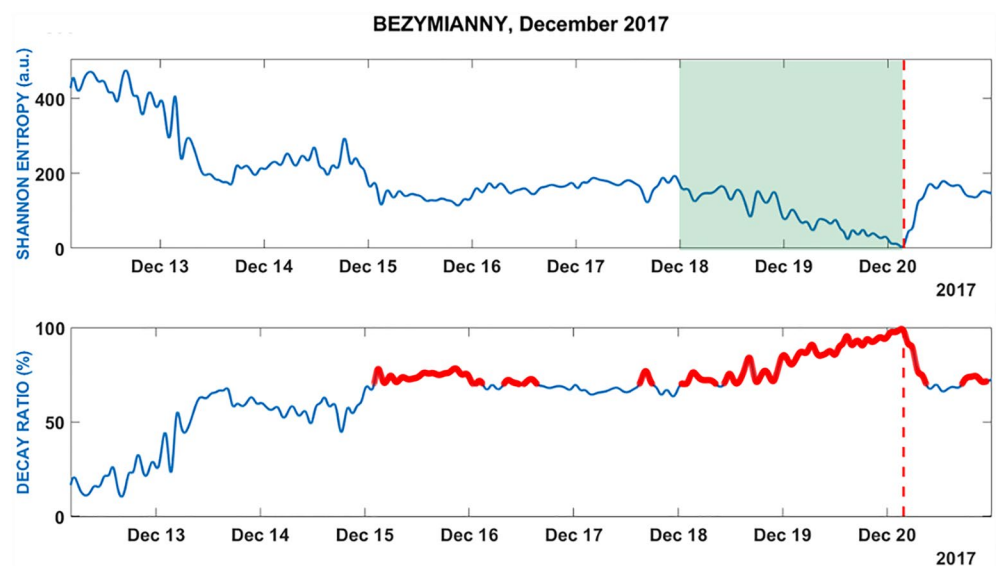


Figure 4. (Up) Temporal evolution of the Shannon entropy before and after eruptive episode of Bezymianny, December 2017 marked with a vertical red line. Green region indicates a stable decay bigger than the 70%. Decay at the moment of the eruption: 98.3%. (Down) Temporal evolution of the Short Time Average/Long Time Average ratio making in red values bigger than 70%.

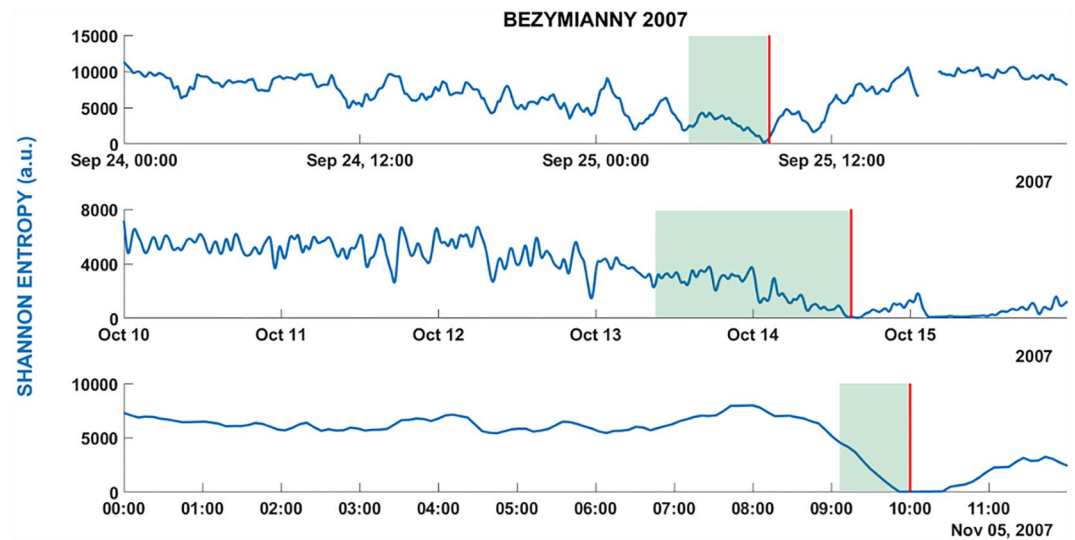


Figure 5. Temporal evolution of the Shannon entropy before and after three explosive episodes of Bezymianny in 2007, all of them marked with vertical red lines. Green region indicates a decay bigger than the 70%. Decay at the moment of the eruption: 99.5%, 99.5% and 100%.

in all cases there were a minimum value of the Shannon entropy at the instant of the volcanic explosion (marked with a red line). These decays were of 99.5%, 99.5%, and 100% respectively. Notice as the pre-eruptive forecasting interval change according each explosion, from 1 hr to a day. According the analysis of Bueno et al. (2021a, 2021b) it seems to be a direct relationship pre-eruptive forecasting interval duration and energy of the explosion, since the larger explosion occurred on 14 October 2007 and it has the longest pre-eruptive evidences.

The analysis of the four lava fountain episodes recorded at Mt. Etna in November 2013 is plotted in Figure 6. As noticed in the precedent analysis we observed a significant decrease (below the marked threshold) prior every paroxysm. In all cases, as in Bezymianny, just when the Shannon entropy start to decrease below the threshold, this is a stable decreasing tendency marking without doubts that some volcanic energetic process will happen, reaching its minimum at the moment of every eruptive episode (in this case lava fountains, marked in red), 98.4%, 98.9%, 97.4%, and 95.1% respectively. The short-term pre-eruptive intervals were 12, 18, 3, and 2 hr respectively and according again with the size of each volcanic episode.

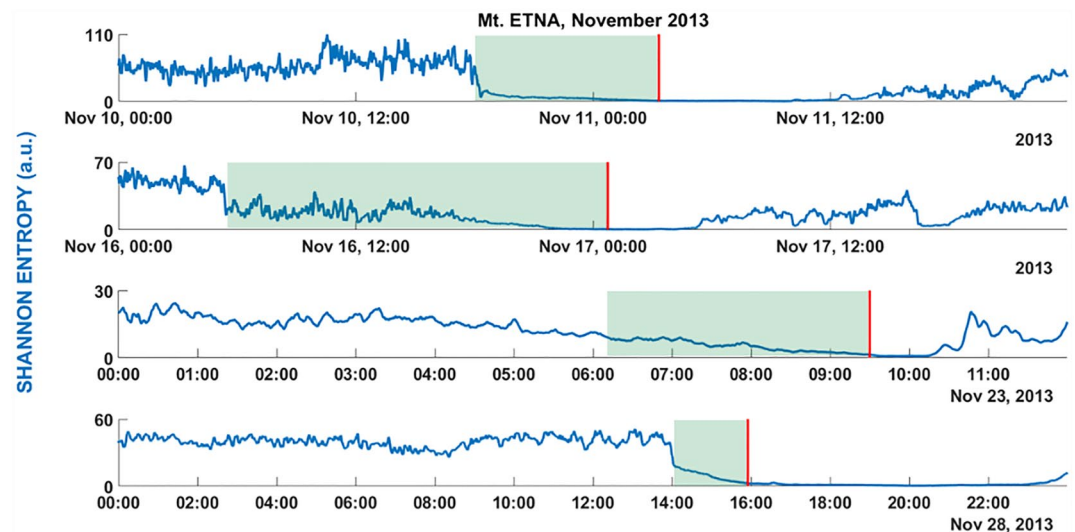


Figure 6. Temporal evolution of the Shannon entropy before and after four lava fountain paroxysms of Mt. Etna during November 2013 all of them marked with vertical red lines. Green region indicates a decay bigger than the 70%. Decay at the moment of the eruption: 98.4%, 98.9%, 97.4%, and 95.1%.

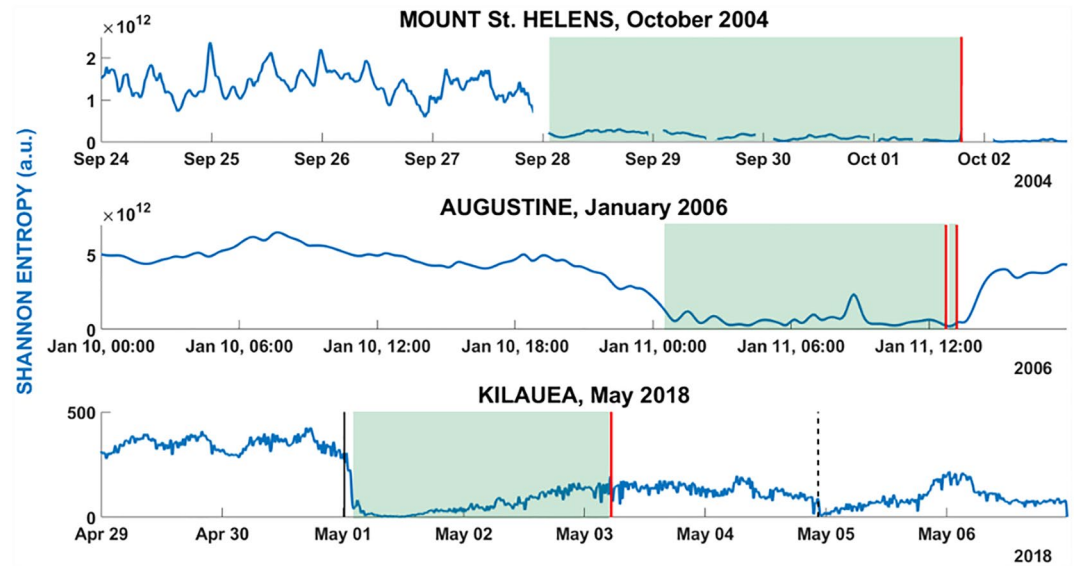


Figure 7. (a) Temporal evolution of the Shannon entropy before and after the 1 October 2004, eruptive episode of Mount St. Helens marked with the vertical red line. Blank spaces in the graph represent data gaps; the vertical red line denote the time of the eruption. (b) Temporal evolution of the Shannon entropy before and after the 11 January 2006, eruption of Augustine. The two main explosions are marked with vertical red lines. (c) Temporal evolution of energy (blue line) and Shannon entropy (orange line) at Kilauea from 29 April to 7 May 2018. The solid black line marks the caldera collapse and the dashed line marks a local Mw 6.9 earthquake. The solid red line denotes the start of the eruptive episode. Green region indicates a decay bigger than the 70%. Decay at the moment of the eruption in Mount St. Helens and Augustine: 100% and 96.8%. Kilauea: induced by summit collapse (99.1%), first fissure (80.7%) and earthquake (98.0%).

Finally, we applied the procedure to the rest of the volcanic scenarios (Mount St. Helens, Augustine, and Kilauea), plotted in Figure 7. In the case of Mount St. Helens and Augustine the decay of the Shannon entropy is 100% and 96.8% respectively. Noteworthy, as indicated above, the analyzed Augustine eruption is characterized by two moderate/large explosions (marked in Figure 7 with two red lines). The proposed approach identifies well the instant of the first explosion with the highest decay of the Shannon entropy value. Their respective short-term forecasting intervals were 4 days and 12 hr. The case of Kilauea is much more complex, observing different decays according the three different processes described above. The decay of the Shannon entropy reaches 99.1% when the summit collapsed, 80.7% when the first fissure and lava flow appeared, and 98.0% when the 6.9 Mw earthquake occurred. There is no measurable forecasting interval for the collapse of the summit and the potential failure of this decay will be discussed in next section.

Thus, we propose, according to Ardid et al. (2022), Shannon entropy is a short-term eruptive precursor, and demonstrated to be recurrent (occurs prior to every eruption studied), transferable (occurs in different volcanoes with different pre-eruptive behavior) and differentiable, as it only changes whenever an eruption occurs, as we conclude after analyzing a year of data recorded continuously.

5. Discussion

After studying five different volcanoes with different eruptive sources, lava types and pre-eruptive behavior we demonstrated the Shannon entropy approach works efficiently as short-term volcanic eruption forecasting tool independently of the eruptive mechanism. In addition, it is interesting to notice each volcanic process studied is dominated for different pre-eruptive type of seismic signals. We have examples of eruptions driven by volcano-tectonic events, like Bezymianny 2017 (Koulakov et al., 2021); others by mainly volcanic tremor like Mt. Etna (Spampinato et al., 2019) or another like Mount St. Helens with the presence of mixed seismicity, first intense swarm of volcano-tectonic events and later by volcanic tremor (Lehto et al., 2010). In order to quantify objectively the evolution of the Shannon entropy and therefore to use it as an accurate short-term forecast volcanic eruptions tool we used an STA/LTA algorithm quantifying the decay ratio. This procedure permits to objectively identify the time intervals in which we can consider we are in a pre-eruptive period. That is, we can

obtain a pre-eruptive indicator without knowing what is the physical mechanism that dominates the eruption, without having previously trained the system for each different eruptive scenario, and of easy integration in the procedures of surveillance in real time.

It is interesting to combine our results with another pre-eruptive seismic evidences to better understand their physical meaning. As Kilburn (2018) indicated ground deformation, volcanic seismicity (mainly VT events) and their associated energy release could be considered one of the most reliable pre-eruptive evidences. As is broadly known, scientific community has been using the energy of the seismic signal to forecast volcanic eruptions (Boué et al., 2016; Ortiz et al., 2003; Power et al., 2013) and recently some variations of the use of the energy have obtained promising results (Caudron et al., 2021; Dempsey et al., 2020, 2022). Despite of several successfully results, some limitations were found. For example, the energy reflects the size of the seismicity prior to an eruption; more energetic events will display bigger energy values independently if they are directly linked with the eruptive process. In addition, the energy is a growing parameter and to determine its maximum or its exactly timing relationship when the eruption will happen is a complex task.

In some volcanoes it is possible to access to seismic catalogs and perform additional analysis on the registered seismicity. We have evidences that some seismic features (see Supporting Information S1) are directly related to the type of seismicity, and therefore to the earthquake-volcanic source. These features can reflect changes in the seismic signal patterns, and they could be associated with possible physical models. Thus, to analyze these patterns we transform the original features vector into a features matrix, as highlighted in Figure 1. As Bueno et al. (2021a, 2021b) and Cortés et al. (2015) indicated, the Kurtosis and the Frequency Index can be used as indicators of the type of recorded seismic events and their evolution according changes in the volcanic system. The Kurtosis (Equation 3) evaluates how the frequencies of the signal are distributed, and the Frequency Index (Equation 4) takes into consideration the ratio of the energy content between high and low frequencies of the signal (we considered low frequencies between 1 and 6 Hz, and high frequencies between 6 and 16 Hz). Therefore, their changes can be directly associated to changes or evolution in the seismic sources.

$$KUR = \frac{1}{n} \sum_i \left(\frac{S[i] - \mu_s}{\sigma_s} \right)^4 \quad (3)$$

$$FI = \log_{10} \left(\frac{E_{\text{high frequencies}}}{E_{\text{low frequencies}}} \right) \quad (4)$$

VT events recorded in a near field have high frequency contains in confront to the background signal, making increase the obtained value of the Kurtosis, as observed by Bueno et al. (2021a). In addition, a shift of the seismic foci from depth to the surface will include an enrichment of the high frequency contains of the signals (since the seismic attenuation will be less effective) showing again increases in the value of the Kurtosis. On the other hand, volcanic tremor is dominated by lower frequency signals (Konstantinou and Schindwein, 2003; Zuccarello et al., 2022). Therefore, the increasing of the volcanic tremor should move the Frequency Index toward negative values in comparison to the background signal. In other word, the kurtosis is more sensitive to the occurrence of VTs and the Frequency Index to the occurrence of volcanic tremor.

To show the relationship between Kurtosis and occurrence of VTs we will study the case of the Bezymianny eruption of 20 December 2017. Koulakov et al. (2021) indicated the occurrence of an intense seismic swarm prior the eruption, however there is no a complete seismic catalog of this period. Using Hidden Markov Model (HMM) we were able to obtain a VT seismic catalog of Bezymianny for the whole month of December 2017 (Benítez et al., 2006; Cortés et al., 2021; Ibáñez et al., 2009). Simultaneously we computed the Kurtosis using the same window length as for the Shannon entropy. In Figure 8 we compare the variations of the Kurtosis and the cumulative number of VTs for intervals 1 hr long. As observed, both evolve in parallel in the days before the eruption. The green shadow area represents the pre-eruptive short-term forecasting interval predicted by the Shannon entropy with the 70% of decay threshold. Notice as these three parameters seem to evolve in a similar way. The advantage to use the seismic features in confront to the identification of seismic events is the faster evaluation procedure and the absence of previous training process (the application of the HMM to obtain a realizable seismic catalog takes longer time). On the other hand, a seismic catalog itself is not a direct eruptive precursor, since it is the input of different precursory algorithms that evaluate the probability of an eruption. However, the evolution of the seismic features could be used directly as precursors.

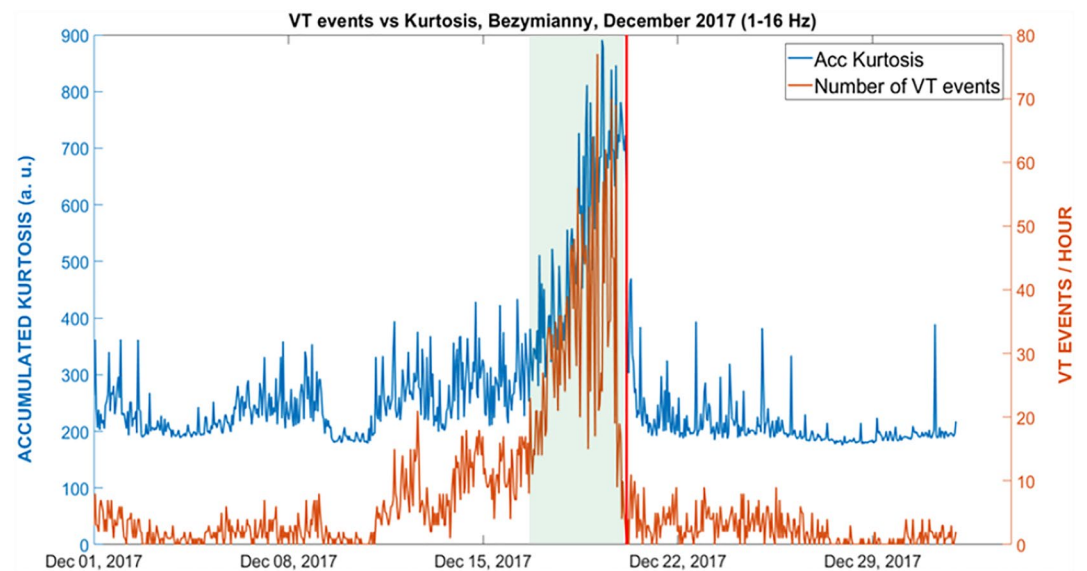


Figure 8. Cumulative number of volcano tectonic earthquakes (orange line) and the temporal evolution of kurtosis (blue line) at station BZ01 of Bezymianny prior to the explosion of 20 December 2017 marked with the vertical red line. Green region indicates a decay of the Shannon entropy larger than the 70%.

However, not all eruptions have VT swarms as precursory activity, as it was the case of the lava fountains of Mt. Etna occurred in 2013. The Frequency Index reflects the temporal variation of the spectral relationship between certain frequency bands, even if it has a complex interpretation. These changes may reflect different volcanic dynamics, both in terms of source and medium; for example, the appearance of VTs, LPs, or tremor could be linked with an increase in the frequency index, and sometimes with a decrease. As the volcano deforms (inflates) prior to an eruption, the increase in system stress will shift the spectral content of the signal toward high frequencies; deflation would shift the spectral content of the signal toward low frequencies (Brenner et al., 2008; Bueno et al., 2019). A change in the impedance contrast at the source, or in the volcanic system, would also cause changes in spectral content. Impedance is the ratio between the elastic properties volcanic fluids and the volcanic edifice (Chouet & Matoza, 2013). Thus, evolution of a resonant system from a “dry” or pure gas to ash-rich content would lead to a shift toward low frequencies, and vice versa. The geometry of the system affects the frequency index, as magma ascends, which is associated to lower frequencies of tremor. In summary, changes in the frequency index are a common pre-eruptive observation, but the style of variation depends on many factors that cannot be controlled a priori, precluding its use in early warning. However, there are “easier” situations as was the case of Mt. Etna in 2013. The volcanic tremor of Mt. Etna uses to appear at frequencies between 1 and 3 Hz (Zuccarello et al., 2022) and the background seismic signal is over 6 Hz (seismic noise). Therefore, it is expected that the Frequency Index must be shifted toward negative values as the volcanic tremor is increasing. In parallel the energy of the seismic signal should increase too. To confirm this hypothesis, we evaluated the temporal evolution of the Frequency Index and the Energy for the Mt. Etna lava fountains and compared them with the evolution of the Shannon entropy (Figure 9).

Notice as when the volcanic tremor appeared we observed a sudden change in both, Shannon entropy (moving toward zero), the Frequency Index (moving toward negative values) and Energy (growing significantly). All used parameters marked a clear pre-event time. However, the Shannon entropy is the only one feature which trend could be associated with the timing of the eruption (marked in the moment of the lower value, 98.4% lower than the LTA). The energy continues growing until the paroxysmal moment of high energetic lava fountain; meanwhile the Frequency Index reveals the different mechanism associated to the eruption and timing of the tremor appearance, with a non-homogeneous pattern.

The two previous examples were dominated by a single type of seismicity, VT events for Bezymianny and volcanic tremor of Mt. Etna. The Mount St. Helens eruption of 2004 is an example of multiple pre-event seismicity, as indicated above. In Figure 10 we plot the temporal evolution of the three features introduced in this section. Green region represents the moment when the Shannon entropy decays over the 70%. The energy starts

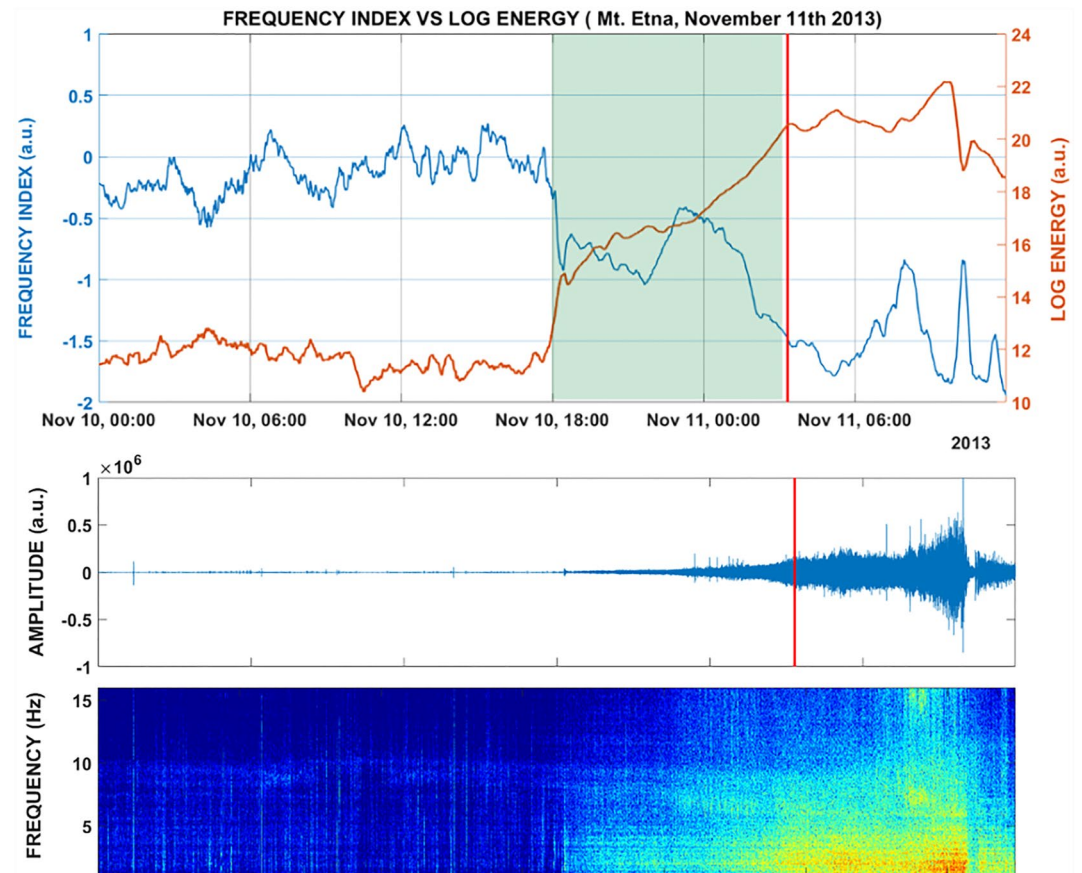


Figure 9. (Upper figure) Comparison between the temporal evolution of the logarithm of the energy (orange line) and the temporal evolution of Frequency Index (blue line) at station EBEM of Mt. Etna prior to the lava fountain of 23 November 2013, marked with the vertical red line. Green region indicates decay of the Shannon entropy bigger than the 70% of the average value until the starting of the eruption. (Lower figure) seismogram and spectrogram of the volcanic tremor associated to the lava fountain eruption.

its growth more than a day and a half later than the instant the Shannon entropy works as short-term forecast indicator. In addition, the energy reaches a maximum and then decrease, without erupting yet. Notice the high values of the cumulative Kurtosis between the days 25 and 28 reflect the high number of VT events detected. Later, the pre-eruptive process starts to be dominated by the volcanic tremor, as reflected by the negative values of the Frequency Index and the decrease of the Kurtosis.

It is noteworthy that kurtosis and the frequency index cannot be used individually as universal predictive elements. However, when combined with the Shannon entropy, they provide information on the type of prevailing seismic activity, the medium, elastic properties, and more; they are therefore useful for investigating the mechanisms of the volcanic source.

Previous studies have shown that entropy can be used to characterize very energetic seismic series or catastrophic energetic events (e.g., Posadas et al., 2021). To identify potential external factors that could affect entropy, we selected a fifth volcanic scenario with complete characteristics—the April–May 2018 eruption of Kilauea. This eruption was preceded by a caldera collapse and subsequent Mw 6.9 earthquake. A proposed triggering mechanism was precipitation (Farquharson & Amelung, 2020), which may have changed the pore pressure in the rift zone. Figure 7c shows Shannon entropy and seismic energy from 29 April to 7 May 2018. Sharp drops, with the values approaching zero, occurred at the same time as (but not before) the caldera collapse and earthquake. Then, during the eruptive episode, Shannon entropy remained very low. As such, Shannon entropy was not a precursory feature.

If rainfall was the eruption trigger, the eruption was not a classic example of an inner-source driven volcanic system, but was a sudden eruptive phenomenon triggered by external factors. This could explain why pre-eruptive

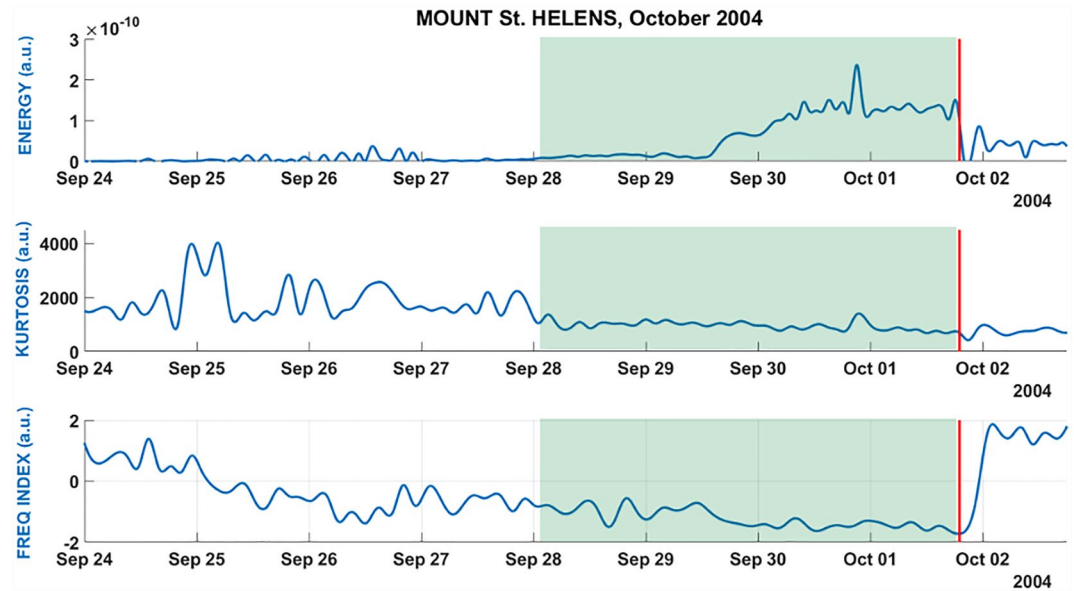


Figure 10. Temporal evolution of energy, kurtosis, and frequency index prior to the eruption of Mount St. Helens, October 2004, marked with the vertical red line. Green region indicates a decay bigger than the 70%.

Shannon entropy was not a suitable precursory indicator for this unrest. Based on this example, we suggest that decreasing Shannon entropy toward zero can only be a precursor for short-term early warning in systems controlled by internal factors; those eruptions triggered by external events (e.g., heavy rainfall) cannot be predicted using this method.

As a resume:

- (a) We observed that in all analyzed volcanic scenarios there is always a quantitatively evaluated decrease of the Shannon entropy prior to different type of eruptions independently of the characteristics of pre-eruptive state and seismic sequences. Therefore, is a good “agnostic” short-term volcanic eruption forecast indicator.
- (b) The Shannon entropy remains high and almost constant when the volcano is resting or when the activity is minor.
- (c) In all cases the energy is a valuable feature to confirm this observation, but it does not always be used as short-term forecasting feature.
- (d) The use of other seismic parameter, such as Kurtosis or Frequency Index, helps to constrain potential physical models driving the eruption.
- (e) We suggest the use of this seismic feature since it is fast and easy to implement, works in real time, it does not need previous training and it is transferable among different volcanoes.

6. Conclusions

The results of this study suggest that the monitoring of Shannon entropy of pre-eruptive seismic signals offers a robust and reliable feature for volcanic eruption early warning. Comparing the energy evolution and the Shannon entropy we can find some interesting features. The main observation is Shannon entropy decays to zero when the system reorganizes itself and the signals are more similar between them, allowing us to easily identify changes in the volcanic system. The relationship between pre-eruptive seismic signals and Shannon entropy is direct and based on changes in the probability distributions of the type of seismic waves, independent of their source. As a uniform volcanic source processes toward an eruption there is high homogeneity of recorded seismic wave types, regardless of the energy and underlying source processes. This homogeneity can be measured quantitatively through the Shannon entropy and the trend toward zero will mark the imminent start of the volcanic eruption.

Combining this with other features, such as energy, Kurtosis, Frequency Index and interesting parameters selected in future works, offers even greater predictive certainty, along with insight into the types of seismic sources and

physical changes in the volcanic system. In general, this approach is exportable from one volcanic system to another. However, it falls short of universality because eruptions triggered by external processes (e.g., rainfall) cannot be predicted in this way. Shannon entropy is simple and rapid to evaluate, and the relevant pre-eruptive changes (i.e., a decrease toward zero) occur over intervals of between 4 days and 12 hr prior to eruption, which is sufficient for the relevant authorities to implement alert and evacuation protocols.

Data Availability Statement

Data of the five volcanoes analyzed in this work are publicly accessible in the links that will be detailed below. The used software of this work (all programmed developed by us) are also publicly accessible (link provided below) and are also presented with specific use examples to be able to independently reproduce all the results obtained in this work. The repository sites used are stable, publicly accessible for free and recognized by the scientific community.

1. Augustine Volcano (2006) data were obtained by using the facilities of IRIS Data Services, and specifically the IRIS Data Management Center. Direct links to access to the data of this volcano are:
<https://ds.iris.edu/mda/AV/>
<https://doi.org/10.7914/SN/II>
<https://ds.iris.edu/mda/HV/JOKA/?starttime=2012-09-17T00:00:00&endtime=2599-12-31T23:59:59>
 In addition data are also available in Alaska Volcano Observatory/USGS (1988). Alaska Volcano Observatory [Dataset]. International Federation of Digital Seismograph Networks. <https://doi.org/10.7914/SN/AV>
 2. Kilauea Volcano (2018) data were obtained by using the facilities of IRIS Data Services, and specifically the IRIS Data Management Center. Direct links to access to the data of this volcano are:
<https://ds.iris.edu/mda/HV/>
<https://doi.org/10.7914/SN/II>
<https://ds.iris.edu/mda/HV/JOKA/?starttime=2012-09-17T00:00:00&endtime=2599-12-31T23:59:59>
 3. Mount St. Helens (2004) data were obtained by using the facilities of IRIS Data Services, and specifically the IRIS Data Management Center. Direct links to access to the data of this volcano are:
<https://ds.iris.edu/mda/UW/>
<https://doi.org/10.7914/SN/II>
<https://ds.iris.edu/mda/UW/SHW/?starttime=1972-10-01T00:00:00&endtime=2599-12-31T23:59:59>
 4. Bezymianny volcano. Data from 2007 were obtained by using the facilities of IRIS Data Services, and specifically the IRIS Data Management Center. Data for the temporary experiment (2017–2018) are available in the compressed folder “Dataset_volcanoes.Rar,” located in the ZENODO repository at the following address and DOI.
<https://doi.org/10.5281/zenodo.6821530>
<https://zenodo.org/record/6821530#.YvyeUS7P1PY>
 5. Etna volcano data (2013) are available in the ZENODO repository at the following address and DOI.
<https://doi.org/10.5281/zenodo.6849621>
<https://zenodo.org/record/6849621#.YvyetS7P1PY>
- (A) Instructions for downloading the data associated with the IRIS network, as well as the access to the download software developed by us, can be found in the “Readme.txt” file, available in the ZENODO repository at the following address and DOI.
<https://doi.org/10.5281/zenodo.6821530>
<https://zenodo.org/record/6821530#.YvyeUS7P1PY>
 - (B) The seismic parameter analysis software, with illustrative examples to be able to reproduce our results, are available in the compressed folder “Software.Rar,” located in the ZENODO repository at the following address and DOI.
<https://doi.org/10.5281/zenodo.6821530>
<https://zenodo.org/record/6821530#.YvyeUS7P1PY>
 - (C) The software related to the automatic recognition of seismic signals used for the study of the Bezymianny volcano is developed under the EU project called VULCAN.ears located in the ZENODO repository at the following address and DOI.

<https://zenodo.org/record/3594080#.YvydiC7P1PY>
<https://zenodo.org/record/4305100#.Yvydti7P1PY>
<https://doi.org/10.5281/zenodo.4305100>

Acknowledgments

We would like to thank the invaluable contribution of the editor Dr. R. Abercrombie, the comments of associated editor, the high quality and complete revision of Dr. Alberto Ardid and the suggestion of an anonymous reviewer that improved the quality of this manuscript. This study was partially supported by the Spanish FEMALE (PID2019-106260GB-I00) and PROOF-FOREVER (EUR2022.134044) projects. P. Rey-Devesa was funded by the Ministerio de Ciencia e Innovación del Gobierno de España (MCIN), Agencia Estatal de Investigación (AEI), Fondo Social Europeo (FSE), and Programa Estatal de Promoción del Talento y su Empleabilidad en I+D+I Ayudas para contratos predoctorales para la formación de doctores 2020 (PRE2020-092719). Ivan Koulikov was supported by the Russian Science Foundation (Grant 20-17-00075). Luciano Zuccarello was supported by the INGV Pianeta Dinamico 2021 Tema 8 SOME project (Grant CUP D53J1900017001) funded by the Italian Ministry of University and Research "Fondo finalizzato al rilancio degli investimenti delle amministrazioni centrali dello Stato e allo sviluppo del Paese, legge 145/2018." Luciano Zuccarello and Jesús Ibáñez were partially funded by the INGV-Italy project "Progetto Pianeta Dinamico 2023, tema VT_DYNAMO." English language editing was performed by Tornillo Scientific, UK. Funding for open access charge: Universidad de Granada/CBUA.

References

- Almendros, J., Ibáñez, J. M., Carmona, E., & Zandomenighi, D. (2007). Array analyses of volcanic earthquakes and tremor recorded at Las Cañadas caldera (Tenerife Island, Spain) during the 2004 seismic activation of Teide volcano. *Journal of Volcanology and Geothermal Research*, *160*(3–4), 285–299. <https://doi.org/10.1016/j.jvolgeores.2006.10.002>
- Aloisi, M., Bonaccorso, A., Cannavò, F., Currenti, G., & Gambino, S. (2020). The 24 December 2018 eruptive intrusion at Etna volcano as revealed by multidisciplinary continuous deformation networks (CGPS, Borehole Strainmeters and Tiltmeters). *Journal of Geophysical Research: Solid Earth*, *125*(8). <https://doi.org/10.1029/2019JB019117>
- Alparone, S., Maiolino, V., Mostaccio, A., Scaltrito, A., Ursino, A., Barberi, G., et al. (2015). Instrumental seismic catalogue of Mt. Etna earthquakes (Sicily, Italy): Ten years (2000–2010) of instrumental recordings. *Annals of Geophysics*, *58*(4). <https://doi.org/10.4401/ag-6591>
- Alvarez, I., Garcia, L., Cortes, G., Benitez, C., & De la Torre, Á. (2011). Discriminative feature selection for automatic classification of volcano-seismic signals. *IEEE Geoscience and Remote Sensing Letters*, *9*(2), 151–155. <https://doi.org/10.1109/LGRS.2011.2162815>
- Anderson, K., & Segal, P. (2013). Bayesian inversion of data from effusive volcanic eruptions using physics-based models: Application to Mount St. Helens 2004–2008. *Journal of Geophysical Research: Solid Earth*, *118*(5), 2017–2037. <https://doi.org/10.1002/jgrb.50169>
- Ardid, A., Dempsey, D., Caudron, C., & Cronin, S. (2022). Seismic precursors to the Whakaari 2019 phreatic eruption are transferable to other eruptions and volcanoes. *Nature Communications*, *13*(1), 1–9. <https://doi.org/10.1038/s41467-022-29681-y>
- Bailey, J. E., Dean, K. G., Dehn, J., Webley, P. W., Power, J., Coombs, M., & Freymueller, J. (2006). Integrated satellite observations of the 2006 eruption of Augustine Volcano. In *The 2006 eruption of Augustine Volcano, Alaska* (pp. 481–506).
- Barreca, G., Branca, S., Corsaro, R. A., Scarfi, L., Cannavò, F., Aloisi, M., et al. (2020). Slab detachment, mantle flow, and crustal collision in eastern Sicily (southern Italy): Implications on Mount Etna volcanism. *Tectonics*, *39*(9). <https://doi.org/10.1029/2020TC006188>
- Barreca, G., Branca, S., & Monaco, C. (2018). Three-dimensional modeling of Mount Etna Volcano: Volume assessment, trend of eruption rates, and geodynamic significance. *Tectonics*, *37*(3), 842–857. <https://doi.org/10.1002/2017TC004851>
- Benítez, M. C., Ramírez, J., Segura, J. C., Ibanez, J. M., Almendros, J., García-Yeguas, A., & Cortes, G. (2006). Continuous HMM-based seismic-event classification at Deception Island, Antarctica. *IEEE Transactions on Geoscience and Remote Sensing*, *45*(1), 138–146. <https://doi.org/10.1109/TGRS.2006.882264>
- Berlo, K., Blundy, J., Turner, S., Cashman, K., Hawkesworth, C., & Black, S. (2004). Geochemical precursors to volcanic activity at Mount St. Helens, USA. *Science*, *306*(5699), 1167–1169. <https://doi.org/10.1126/science.1103869>
- Bonaccorso, A., Calvari, S., Linde, A., & Sacks, S. (2014). Eruptive processes leading to the most explosive lava fountain at Etna volcano: The 23 November 2013 episode. *Geophysical Research Letters*, *41*(14), 4912–4919. <https://doi.org/10.1002/2014GL060623>
- Boué, A., Lesage, P., Cortés, G., Valette, B., & Reyes-Dávila, G. (2015). Real-time eruption forecasting using the material Failure Forecast Method with a Bayesian approach. *Journal of Geophysical Research: Solid Earth*, *120*(4), 2143–2161. <https://doi.org/10.1002/2014JB011637>
- Boué, A., Lesage, P., Cortés, G., Valette, B., Reyes-Dávila, G., Arámbula-Mendoza, R., & Budi-Santoso, A. (2016). Performance of the 'material Failure Forecast Method' in real-time situations: A Bayesian approach applied on effusive and explosive eruptions. *Journal of Volcanology and Geothermal Research*, *327*, 622–633. <https://doi.org/10.1016/j.jvolgeores.2016.10.002>
- Brenguier, F., Shapiro, N. M., Campillo, M., Ferrazzini, V., Duputel, Z., Coutant, O., & Nercessian, A. (2008). Towards forecasting volcanic eruptions using seismic noise. *Nature Geoscience*, *1*(2), 126–130. <https://doi.org/10.1038/ngeo104>
- Bueno, A., Benitez, C., De Angelis, S., Moreno, A. D., & Ibáñez, J. M. (2019). Volcano-seismic transfer learning and uncertainty quantification with Bayesian neural networks. *IEEE Transactions on Geoscience and Remote Sensing*, *58*(2), 892–902. <https://doi.org/10.1109/TGRS.2019.2941494>
- Bueno, A., Benítez, C., Zuccarello, L., De Angelis, S., & Ibáñez, J. M. (2021b). Bayesian monitoring of seismo-volcanic dynamics. *IEEE Transactions on Geoscience and Remote Sensing*, *60*, 1–14. <https://doi.org/10.1109/TGRS.2021.3076012>
- Bueno, A., Titos, M., Benítez, C., & Ibáñez, J. M. (2021a). Continuous active learning for seismo-volcanic monitoring. *IEEE Geoscience and Remote Sensing Letters*, *19*, 1–5. <https://doi.org/10.1109/lgrs.2021.3121611>
- Bueno, A., Titos, M., García, L., Álvarez, I., Ibáñez, J., & Benítez, C. (2018). Classification of volcano-seismic signals with Bayesian neural networks. In *Proceedings of the 26th IEEE European signal processing conference (EUSIPCO)* (pp. 2295–2299).
- Buurman, H., & West, M. E. (2006). Seismic precursors to volcanic explosions during the 2006 eruption of Augustine Volcano. In J. A. Power, M. L. Coombs, & J. T. Freymueller (Eds.), *The 2006 eruption of Augustine Volcano, Alaska* (pp. 41–57). U.S. Geological Survey Professional Paper 1769. Retrieved from https://pubs.usgs.gov/pp/1769/chapters/p1769_chapter02.pdf
- Cameron, C. E., Prejean, S. G., Coombs, M. L., Wallace, K. L., Power, J. A., & Roman, D. C. (2018). Alaska volcano observatory alert and forecasting timeliness: 1989–2017. *Frontiers in Earth Science*, *6*, 86. <https://doi.org/10.3389/feart.2018.00086>
- Caudron, C., Chardot, L., Girona, T., Aoki, Y., & Fournier, N. (2020). Towards improved forecasting of volcanic eruptions. *Frontiers in Earth Science*, *8*, 45. <https://doi.org/10.3389/feart.2020.00045>
- Caudron, C., Girona, T., Jolly, A., Christenson, B., Savage, M. K., Carniel, R., et al. (2021). A quest for unrest in multiparameter observations at Whakaari/White Island volcano, New Zealand 2007–2018. *Earth, Planets and Space*, *73*(1), 1–21. <https://doi.org/10.1186/s40623-021-01506-0>
- Chardot, L., Jolly, A. D., Kennedy, B. M., Fournier, N., & Sherburn, S. (2015). Using volcanic tremor for eruption forecasting at White Island volcano (Whakaari), New Zealand. *Journal of Volcanology and Geothermal Research*, *302*, 11–23. <https://doi.org/10.1016/j.jvolgeores.2015.06.001>
- Chouet, B. A., & Matoza, R. S. (2013). A multi-decadal view of seismic methods for detecting precursors of magma movement and eruption. *Journal of Volcanology and Geothermal Research*, *252*, 108–175. <https://doi.org/10.1016/j.jvolgeores.2012.11.013>
- Coombs, M. L., Bull, K. F., Vallance, J. W., Schneider, D. J., Thoms, E. E., Wessels, R. L., & McGimsey, R. G. (2010). Timing, distribution, and volume of proximal products of the 2006 eruption of Augustine Volcano. In J. A. Power, M. L. Coombs, & J. T. Freymueller (Eds.), *The 2006 eruption of Augustine Volcano, Alaska* (pp. 145–185). U.S. Geological Survey Professional Paper 1769. Retrieved from https://pubs.usgs.gov/pp/1769/chapters/p1769_chapter08/p1769_ch08_text.pdf
- Cornelius, R. R., & Voight, B. (1995). Seismological aspects of the 1989–1990 eruption at Redoubt Volcano, Alaska: The Materials Failure Forecast Method (FFM) with RSAM and SSAM seismic data. *Journal of Volcanology and Geothermal Research*, *62*(1–4), 469–498. [https://doi.org/10.1016/0377-0273\(94\)00078-U](https://doi.org/10.1016/0377-0273(94)00078-U)

- Cortés, G., Arámbula, R., Gutiérrez, L., Benítez, C., Ibáñez, J., Lesage, P., et al. (2009). Evaluating robustness of a HMM-based classification system of volcano-seismic events at Colima and Popocatepetl volcanoes. In *Proceedings of the 2009 IEEE International Geoscience and Remote Sensing Symposium* (Vol. 2, pp. II-1012).
- Cortés, G., Benítez, M. C., García, L., Álvarez, I., & Ibanez, J. M. (2015). A comparative study of dimensionality reduction algorithms applied to volcano-seismic signals. *IEEE Journal of Selected Topics in Applied Earth Observations and Remote Sensing*, 9(1), 253–263. <https://doi.org/10.1109/JSTARS.2015.2479300>
- Cortés, G., Carniel, R., Lesage, P., Mendoza, M. Á., & Della Lucia, I. (2021). Practical volcano-independent recognition of seismic events: VULCAN. Ears project. *Frontiers in Earth Science*, 8, 616676. <https://doi.org/10.3389/feart.2020.616676>
- Cortés, G., Carniel, R., Mendoza, M. Á., & Lesage, P. (2019). Standardization of noisy volcanoseismic waveforms as a key step toward station-independent, robust automatic recognition. *Seismological Research Letters*, 90(2A), 581–590. <https://doi.org/10.1785/0220180334>
- Cortés, G., García, L., Álvarez, I., Benítez, C., de la Torre, Á., & Ibáñez, J. (2014). Parallel system architecture (PSA): An efficient approach for automatic recognition of volcano-seismic events. *Journal of Volcanology and Geothermal Research*, 271, 1–10. <https://doi.org/10.1016/j.jvolgeores.2013.07.004>
- Davydova, V. O., Shcherbakov, V. D., Plechov, P. Y., & Koulov, I. Y. (2022). Petrological evidence of rapid evolution of the magma plumbing system of Bezymianny volcano in Kamchatka before the December 20th, 2017 eruption. *Journal of Volcanology and Geothermal Research*, 421, 107422. <https://doi.org/10.1016/j.jvolgeores.2021.107422>
- Dempsey, D. E., Cronin, S. J., Mei, S., & Kempa-Liehr, A. W. (2020). Automatic precursor recognition and real-time forecasting of sudden explosive volcanic eruptions at Whakaari, New Zealand. *Nature Communications*, 11(1), 1–8. <https://doi.org/10.1038/s41467-020-17375-2>
- Dempsey, D. E., Kempa-Liehr, A. W., Ardid, A., Li, A., Orenia, S., Singh, J., et al. (2022). Evaluation of short-term probabilistic eruption forecasting at Whakaari, New Zealand. *Bulletin of Volcanology*, 84(10), 91. <https://doi.org/10.1007/s00445-022-01600-5>
- DeRoin, N., & McNutt, S. R. (2012). Rockfalls at Augustine Volcano, Alaska: The influence of eruption precursors and seasonal factors on occurrence patterns 1997–2009. *Journal of Volcanology and Geothermal Research*, 211, 61–75. <https://doi.org/10.1016/j.jvolgeores.2011.11.0>
- DeShon, H. R., Thurber, C. H., & Power, J. A. (2010). Earthquake waveform similarity and evolution at Augustine Volcano from 1993 to 2006. In J. A. Power, M. L. Coombs, & J. T. Freymueller (Eds.), *The 2006 eruption of Augustine Volcano, Alaska* (pp. 103–118). U.S. Geological Survey Professional Paper 1769. Retrieved from https://pubs.usgs.gov/pp/1769/chapters/p1769_chapter05.pdf
- De Siena, L., Thomas, C., Waite, G. P., Moran, S. C., & Klemme, S. (2014). Attenuation and scattering tomography of the deep plumbing system of Mount St. Helens. *Journal of Geophysical Research: Solid Earth*, 119(11), 8223–8238. <https://doi.org/10.1002/2014JB011372>
- Endo, E. T., & Murray, T. (1991). Real-time seismic amplitude measurement (RSAM): A volcano monitoring and prediction tool. *Bulletin of Volcanology*, 53(7), 533–545. <https://doi.org/10.1007/BF00298154>
- Esmaili, S., Krishnan, S., & Raahemifar, K. (2004). Content based audio classification and retrieval using joint time-frequency analysis. In *Proceedings of the 2004 IEEE International Conference on Acoustics, Speech, and Signal Processing* (Vol. 5, pp. V-665).
- Farquharson, J. I., & Amelung, F. (2020). Extreme rainfall triggered the 2018 rift eruption at Kilauea Volcano. *Nature*, 580(7804), 491–495. <https://doi.org/10.1038/s41586-020-2172-5>
- Freire, S., Florczyk, A. J., Pesaresi, M., & Sliuzas, R. (2019). An improved global analysis of population distribution in proximity to active volcanoes, 1975–2015. *ISPRS International Journal of Geo-Information*, 8(8), 341. <https://doi.org/10.3390/ijgi8080341>
- Gabrielli, S., De Siena, L., Napolitano, F., & Del Pezzo, E. (2020). Understanding seismic path biases and magmatic activity at Mount St Helens volcano before its 2004 eruption. *Geophysical Journal International*, 222(1), 169–188. <https://doi.org/10.1093/gji/ggaa154>
- Girina, O. A. (2013). Chronology of Bezymianny volcano activity, 1956–2010. *Journal of Volcanology and Geothermal Research*, 263, 22–41. <https://doi.org/10.1016/j.jvolgeores.2013.05.002>
- Girona, T., Caudron, C., & Huber, C. (2019). Origin of shallow volcanic tremor: The dynamics of gas pockets trapped beneath thin permeable media. *Journal of Geophysical Research: Solid Earth*, 124(5), 4831–4861. <https://doi.org/10.1029/2019JB017482>
- Girona, T., Realmuto, V., & Lundgren, P. (2021). Large-scale thermal unrest of volcanoes for years prior to eruption. *Nature Geoscience*, 14(4), 238–241. <https://doi.org/10.1038/s41561-021-00705-4>
- Ibáñez, J. M., Benítez, C., Gutiérrez, L. A., Cortés, G., García-Yeguas, A., & Alguacil, G. (2009). The classification of seismo-volcanic signals using Hidden Markov Models as applied to the Stromboli and Etna volcanoes. *Journal of Volcanology and Geothermal Research*, 187(3–4), 218–226. <https://doi.org/10.1016/j.jvolgeores.2009.09.002>
- Ibáñez, J. M., Pezzo, E. D., Almendros, J., La Rocca, M., Alguacil, G., Ortiz, R., & García, A. (2000). Seismovolcanic signals at Deception Island volcano, Antarctica: Wave field analysis and source modeling. *Journal of Geophysical Research*, 105(B6), 13905–13931. <https://doi.org/10.1029/2000jb900013>
- Iverson, R. M., Dzurisin, D., Gardner, C. A., Gerlach, T. M., LaHusen, R. G., Lisowski, M., et al. (2006). Dynamics of seismogenic volcanic extrusion at Mount St Helens in 2004–05. *Nature*, 444(7118), 439–443. <https://doi.org/10.1038/nature05322>
- Jolly, A., Caudron, C., Girona, T., Christenson, B., & Carniel, R. (2020). ‘Silent’ dome emplacement into a wet volcano: Observations from an effusive eruption at White Island (Whakaari), New Zealand in late 2012. *Geosciences*, 10(4), 142. <https://doi.org/10.3390/geosciences10040142>
- Jones, J. P., & van der Baan, M. (2015). Adaptive STA–LTA with outlier statistics. *Bulletin of the Seismological Society of America*, 105(3), 1606–1618. <https://doi.org/10.1785/0120140203>
- Kilburn, C. R. (2018). Forecasting volcanic eruptions: Beyond the failure forecast method. *Frontiers in Earth Science*, 133. <https://doi.org/10.3389/feart.2018.00133>
- Kilburn, C. R. J., & Bell, A. F. (2022). Forecasting eruptions from long-quietcent volcanoes. *Bulletin of Volcanology*, 84(3), 25. <https://doi.org/10.1007/s00445-022-01532-0>
- Konstantinou, K. I., & Schlindwein, V. (2003). Nature, wavefield properties and source mechanism of volcanic tremor: A review. *Journal of Volcanology and Geothermal Research*, 119(1–4), 161–187. [https://doi.org/10.1016/s0377-0273\(02\)00311-6](https://doi.org/10.1016/s0377-0273(02)00311-6)
- Koulov, I., Plechov, P., Mania, R., Walter, T. R., Smirnov, S. Z., Abkadyrov, I., et al. (2021). Anatomy of the Bezymianny volcano merely before an explosive eruption on 20.12. 2017. *Scientific Reports*, 11(1), 1–12. <https://doi.org/10.1038/s41598-021-81498-9>
- Lehto, H. L., Roman, D. C., & Moran, S. C. (2010). Temporal changes in stress preceding the 2004–2008 eruption of Mount St. Helens, Washington. *Journal of Volcanology and Geothermal Research*, 198(1–2), 129–142. <https://doi.org/10.1016/j.jvolgeores.2010.08.015>
- Malfante, M., Dalla Mura, M., Mars, J. I., Métaixian, J. P., Macedo, O., & Inza, A. (2018). Automatic classification of volcano seismic signatures. *Journal of Geophysical Research: Solid Earth*, 123(12), 10645–10658. <https://doi.org/10.1029/2018JB015470>
- Malfante, M., Dalla Mura, M., Métaixian, J. P., Mars, J. I., Macedo, O., & Inza, A. (2018). Machine learning for volcano-seismic signals: Challenges and perspectives. *IEEE Signal Processing Magazine*, 35(2), 20–30. <https://doi.org/10.1109/MSP.2017.2779166>
- Manga, M., Carn, S. A., Cashman, K. V., Clarke, A. B., Connor, C. B., Cooper, K. M., et al. (2017). *Volcanic eruptions and their repose, unrest, precursors, and timing*. National Academies Press. <https://doi.org/10.17226/24650>

- Mania, R., Walter, T. R., Belousova, M., Belousov, A., & Senyukov, S. L. (2019). Deformations and morphology changes associated with the 2016–2017 eruption sequence at Bezymianny Volcano, Kamchatka. *Remote Sensing*, *11*(11), 1278. <https://doi.org/10.3390/rs11111278>
- Manley, G. F., Mather, T. A., Pyle, D. M., Clifton, D. A., Rodgers, M., Thompson, G., & Roman, D. C. (2021). Machine learning approaches to identifying changes in eruptive state using multi-parameter datasets from the 2006 eruption of Augustine Volcano, Alaska. *Journal of Geophysical Research: Solid Earth*, *126*(12), e2021JB022323. <https://doi.org/10.1029/2021JB022323>
- Manley, G. F., Pyle, D. M., Mather, T. A., Rodgers, M., Clifton, D. A., Stokell, B. G., et al. (2020). Understanding the timing of eruption end using a machine learning approach to classification of seismic time series. *Journal of Volcanology and Geothermal Research*, *401*, 106917. <https://doi.org/10.1016/j.jvolgeores.2020.1069>
- Martínez, V. L., Titos, M., Benítez, C., Badi, G., Casas, J. A., Craig, V. H. O., & Ibañez, J. M. (2021). Advanced signal recognition methods applied to seismo-volcanic events from Planchon Peteroa Volcanic Complex: Deep Neural Network classifier. *Journal of South American Earth Sciences*, *107*(1–12), 103115. <https://doi.org/10.1016/j.jsames.2020.103115>
- Massa, B., D'Auria, L., Cristiano, E., & De Matteo, A. (2016). Determining the stress field in active volcanoes using focal mechanisms. *Frontiers in Earth Science*, *4*, 103. <https://doi.org/10.3389/feart.2016.00103>
- McKee, K., Smith, C. M., Reath, K., Snee, E., Maher, S., Matoza, R. S., et al. (2021a). Evaluating the state-of-the-art in remote volcanic eruption characterization Part I: Raikoke volcano, Kuril Islands. *Journal of Volcanology and Geothermal Research*, *419*, 107354. <https://doi.org/10.1016/j.jvolgeores.2021.107354>
- McKee, K., Smith, C. M., Reath, K., Snee, E., Maher, S., Matoza, R. S., et al. (2021b). Evaluating the state-of-the-art in remote volcanic eruption characterization Part II: Ulawun volcano, Papua New Guinea. *Journal of Volcanology and Geothermal Research*, *420*, 107381. <https://doi.org/10.1016/j.jvolgeores.2021.107381>
- McNutt, S. R., & Roman, D. C. (2015). Volcanic seismicity. In H. Sigurdsson (Ed.), *The encyclopedia of volcanoes* (2nd ed., pp. 1011–1034). Elsevier Inc. <https://doi.org/10.1016/b978-0-12-385938-9.00059-6>
- Neal, C. A., Brantley, S. R., Antolik, L., Babb, J. L., Burgess, M., Calles, K., et al. (2019). The 2018 rift eruption and summit collapse of Kīlauea volcano. *Science*, *363*(6425), 367–374. <https://doi.org/10.1126/science.aav7046>
- Ortiz, R., Moreno, H., Garcia, A., Fuentealba, G., Astiz, M., Peña, P., et al. (2003). Villarrica volcano (Chile): Characteristics of the volcanic tremor and forecasting of small explosions by means of a material failure method. *Journal of Volcanology and Geothermal Research*, *128*(1–3), 247–259. [https://doi.org/10.1016/S0377-0273\(03\)00258-0](https://doi.org/10.1016/S0377-0273(03)00258-0)
- Patrick, M. R., Houghton, B. F., Anderson, K. R., Poland, M. P., Montgomery-Brown, E., Johanson, I., et al. (2020). The cascading origin of the 2018 Kīlauea eruption and implications for future forecasting. *Nature Communications*, *11*(1), 1–13. <https://doi.org/10.1038/s41467-020-19190-1>
- Posadas, A., Morales, J., Ibañez, J. M., & Posadas-Garzon, A. (2021). Shaking Earth: Non-linear seismic processes and the second law of thermodynamics: A case study from Canterbury (New Zealand) earthquakes. *Chaos, Solitons & Fractals*, *151*, 111243. <https://doi.org/10.1016/j.chaos.2021.111243>
- Power, J. A., Coombs, M. L., & Freymueller, J. T. (Eds.) (2010). *The 2006 eruption of Augustine Volcano, Alaska*, 1 plate, scale 1:20,000, and data files. U.S. Geological Survey Professional Paper 1769.(
- Power, J. A., Haney, M. M., Botnick, S. M., Dixon, J. P., Fee, D., Kaufman, A. M., et al. (2020). Goals and development of the Alaska Volcano Observatory seismic network and application to forecasting and detecting volcanic eruptions. *Seismological Research Letters*, *91*(2A), 647–659. <https://doi.org/10.1785/0220190216>
- Power, J. A., Stihler, S. D., Chouet, B. A., Haney, M. M., & Ketner, D. M. (2013). Seismic observations of Redoubt Volcano, Alaska—1989–2010 and a conceptual model of the Redoubt magmatic system. *Journal of Volcanology and Geothermal Research*, *259*, 31–44. <https://doi.org/10.1016/j.jvolgeores.2012.09.014>
- Presti, D. L., Riggì, F., Ferlito, C., Bonanno, D. L., Bonanno, G., Gallo, G., et al. (2020). Muographic monitoring of the volcano-tectonic evolution of Mount Etna. *Scientific Reports*, *10*(1), 1–11. <https://doi.org/10.1038/s41598-020-68435-y>
- Pyle, D. M. (2015). Sizes of volcanic eruptions. In H. Sigurdsson (Ed.), *The encyclopedia of volcanoes* (2nd ed., pp. 257–264). Elsevier. <https://doi.org/10.1016/B978-0-12-385938-9.00013-4>
- Ren, C. X., Peltier, A., Ferrazzini, V., Rouet-Leduc, B., Johnson, P. A., & Brenguier, F. (2020). Machine learning reveals the seismic signature of eruptive behavior at Piton de la Fournaise volcano. *Geophysical Research Letters*, *47*(3), e2019GL085523. <https://doi.org/10.1029/2019GL085523>
- Roman, D. C., Soldati, A., Dingwell, D. B., Houghton, B. F., & Shiro, B. R. (2021). Earthquakes indicated magma viscosity during Kīlauea's 2018 eruption. *Nature*, *592*(7853), 237–241. <https://doi.org/10.1038/s41586-021-03400-x>
- Saccorotti, G., & Lokmer, I. (2021). A review of seismic methods for monitoring and understanding active volcanoes. In P. Papale (Ed.), *Forecasting and planning for volcanic hazards, risks, and disasters* (Vol. 2, pp. 25–73). Elsevier Inc. <https://doi.org/10.1016/b978-0-12-818082-2.00002-0>
- Sherrod, D. R., Scott, W. E., & Stauffer, P. H. (Eds.) (2008). *A volcano rekindled: the renewed eruption of Mount St. Helens, 2004–2006*. U.S. Geological Survey Professional Paper 1750.
- Spampinato, S., Langer, H., Messina, A., & Falsaperla, S. (2019). Short-term detection of volcanic unrest at Mt. Etna by means of a multi-station warning system. *Scientific Reports*, *9*(1), 1–10. <https://doi.org/10.1038/s41598-019-42930-3>
- Sparks, R. S. J. (2003). Forecasting volcanic eruptions. *Earth and Planetary Science Letters*, *210*(1–2), 1–15. [https://doi.org/10.1016/S0012-821X\(03\)00124-9](https://doi.org/10.1016/S0012-821X(03)00124-9)
- Sparks, R. S. J., Biggs, J., & Neuberg, J. W. (2012). Monitoring volcanoes. *Science*, *335*(6074), 1310–1311. <https://doi.org/10.1126/science.1219485>
- Thelen, W., West, M., & Senyukov, S. (2010). Seismic characterization of the fall 2007 eruptive sequence at Bezymianny Volcano, Russia. *Journal of Volcanology and Geothermal Research*, *194*(4), 201–213. <https://doi.org/10.1016/j.jvolgeores.2010.05.010>
- Thelen, W. A., Matoza, R. S., & Hotovec-Ellis, A. J. (2022). Trends in volcano seismology: 2010 to 2020 and beyond. *Bulletin of Volcanology*, *84*(3), 26. <https://doi.org/10.1007/s00445-022-01530-2>
- Titos, M., García, L., Kowsari, M., & Benítez, C. (2022). Toward knowledge extraction in classification of volcano-seismic events: Visualizing hidden states in recurrent neural networks. *IEEE Journal of Selected Topics in Applied Earth Observations and Remote Sensing*, *15*, 2311–2325. <https://doi.org/10.1109/JSTARS.2022.3155967>
- Titos, M., Bueno, A., García, L., & Benítez, C. (2018). A deep neural networks approach to automatic recognition systems for volcano-seismic events. *IEEE Journal of Selected Topics in Applied Earth Observations and Remote Sensing*, *11*(5), 1533–1544. <https://doi.org/10.1109/JSTARS.2018.2803198>
- Titos, M., Bueno, A., García, L., Benítez, C., & Segura, J. C. (2019). Classification of isolated volcano-seismic events based on inductive transfer learning. *IEEE Geoscience and Remote Sensing Letters*, *17*(5), 869–873. <https://doi.org/10.1109/LGRS.2019.2931063>
- Titos, M., Bueno, A., García, L., Benítez, M. C., & Ibañez, J. (2018). Detection and classification of continuous volcano-seismic signals with recurrent neural networks. *IEEE Transactions on Geoscience and Remote Sensing*, *57*(4), 1936–1948. <https://doi.org/10.1109/TGRS.2018.2870202>

- Trnkoczy, A. (2009). Understanding and parameter setting of STA/LTA trigger algorithm. In *New manual of seismological observatory practice (NMSOP)* (pp. 1–20). Deutsches GeoForschungsZentrum GFZ.
- Trujillo-Castrillón, N., Valdés-González, C. M., Arámbula-Mendoza, R., & Santacoloma-Salguero, C. C. (2018). Initial processing of volcanic seismic signals using Hidden Markov Models: Nevado del Huila, Colombia. *Journal of Volcanology and Geothermal Research*, *364*, 107–120. <https://doi.org/10.1016/j.jvolgeores.2018.09.008>
- van Ruitenbeek, F. J., Goseling, J., Bakker, W. H., & Hein, K. A. (2020). Shannon entropy as an indicator for sorting processes in hydrothermal systems. *Entropy*, *22*(6), 656. <https://doi.org/10.3390/e22060656>
- Whitehead, M. G., & Bebbington, M. S. (2021). Method selection in short-term eruption forecasting. *Journal of Volcanology and Geothermal Research*, *419*, 107386. <https://doi.org/10.1016/j.jvolgeores.2021.107386>
- Zhan, Y., Le Mével, H., Roman, D. C., Girona, T., & Gregg, P. M. (2022). Modeling deformation, seismicity, and thermal anomalies driven by degassing during the 2005–2006 pre-eruptive unrest of Augustine Volcano, Alaska. *Earth and Planetary Science Letters*, *585*, 117524. <https://doi.org/10.1016/j.epsl.2022.117524>
- Zuccarello, L., De Angelis, S., Minio, V., Saccorotti, G., Bean, C. J., Paratore, M., & Ibanez, J. M. (2022). Volcanic tremor tracks changes in multi-vent activity at Mt. Etna, Italy: Evidence from analyses of seismic array data. *Geophysical Research Letters*, *49*(22), e2022GL100056. <https://doi.org/10.1029/2022gl100056>